

Innovations in seafood freshness quality: Non-destructive detection of freshness in *Litopenaeus vannamei* using the YOLO-shrimp model

Mingxin Hou^{a,b}, Xiaowen Zhong^c, Ouyang Zheng^{c,*}, Qinxiu Sun^c, Shucheng Liu^c, Mingxin Liu^{b,d}

^a School of Mechanical Engineering, Guangdong Ocean University, Zhanjiang, Guangdong Province, 524088, China

^b Guangdong Provincial Key Laboratory of Intelligent Equipment for South China Sea Marine Ranching, Guangdong Ocean University, Zhanjiang 524088, China

^c College of Food Science and Technology, Guangdong Ocean University, Zhanjiang, Guangdong Province, 524088, China

^d School of Electronics and Information Engineering, Guangdong Ocean University, Zhanjiang, Guangdong Province, 524088, China

ARTICLE INFO

Keywords:

Litopenaeus vannamei
Freshness detection
YOLO shrimp model
Non-destructive detection
Food safety technology

ABSTRACT

The relationship between freshness changes and visual images of *Litopenaeus vannamei* was established based on Sensory Evaluation, Total Volatile Base Nitrogen (TVB-N), Total Viable Count (TVC), and Gray Value during storage at 4 °C. A non-destructive detection system using the advanced YOLO(You Only Look Once)-Shrimp model was developed to evaluate shrimp freshness. The results revealed a gradual increase in freshness indices over time, with the gray value showing strong positive correlations with TVB-N and TVC (0.88 and 0.81). The advanced YOLO-Shrimp model demonstrated notable performance enhancements over the YOLOv8 model, as evidenced by a precision increase of 5.07 %, a recall improvement of 1.58 %, a 3.25 % rise in the F1 score, and a 2.84 % elevation in mAP50. This innovative approach offers substantial potential for enhancing food safety and quality control in the seafood industry.

1. Introduction

Shrimp was a pivotal role in global seafood consumption, with *Litopenaeus vannamei* accounting for 62.2 % of the total shrimp production, reaching an annual output of 7.934 million tons, and had been captivating consumers worldwide due to its rich nutritional value and distinctive flavor (The State of World Fisheries and Aquaculture 2024: Blue Transformation in Action). The preservation of shrimp during storage poses significant challenges due to their high protein and moisture content, along with the various active enzymes within the shrimp, which can lead to spoilage, melanosis, and a decrease in nutritional and sensory quality (Das & Mishra, 2023). The assessment of shrimp freshness is crucial for the identification and grading of shrimp quality, providing a reference for subsequent processing. Traditional biochemical indicators, such as Total Volatile Basic Nitrogen (TVB-N) and Total Viable Count (TVC), are commonly used to gauge freshness. Specifically, TVB-N levels exceeding 30 mg/100 g, as stipulated by the National Food Safety Standard for Fresh and Frozen Aquatic Products (GB 2733-2015), indicate inedibility. However, traditional biochemical methodologies, while accurate, are often encumbered by the necessity

for sample destruction, reliance on large-scale instrumentation, and protracted timelines. For instance, the quantification of TVB-N commonly requires the deployment of an automated Kjeldahl nitrogen analyzer, a device noted for its substantial size and the invasive nature of its analytical process. The assessment of TVC also depends on the use of colony counters and incubators, which are not only labor-intensive but also do not offer the agility needed for expedited, on-site analysis. Moreover, other analytical tools, such as spectrophotometers for tracking absorbance shifts, texture analyzers for evaluating the mechanical attributes of seafood flesh, and electronic noses designed to emulate the detection of volatile organic compounds through olfaction, all present operational complexities and time-intensive procedures. These conventional testing protocols are constrained by their lack of adaptability and their incapability for providing real-time results (Wang et al., 2019). Consequently, there is a pressing demand for the innovation of detection techniques that are non-destructive, expeditious, straightforward, and facile to employ (Wang et al., 2023).

Recent advancements in non-destructive food quality assessment methods have demonstrated significant potential for enhancing freshness detection and quality control, particularly through the integration

* Corresponding author.

E-mail address: zhengouyang07@163.com (O. Zheng).

of electronic noses and surface acoustic wave resonators. For example, surface acoustic wave resonators combined with electronic noses have been effectively used to determine the freshness of Chinese quince (*Cydonia oblonga* Miller) and large yellow croaker (*Pseudosciaena crocea*), achieving high predictive accuracy with regression coefficients of 0.987 and 0.96, respectively (Le et al., 2016; Jian et al., 2016). Additionally, probabilistic neural networks (PNN) combined with electronic noses have shown effective early moldy grain prediction with a discriminating accuracy of 93.75 %, while electronic noses combined with sodium lactate and nisin coatings have provided rapid beef quality evaluation, correlating strongly with key physicochemical indexes (Ying, Liu, & Hui, 2015; Ying, Liu, Hui, & Fu, 2015; Liu et al., 2020). Similarly, non-linear stochastic resonance models have been used to assess litchi freshness and spinyhead croaker fat content, yielding high predictive accuracy and significant linear relationships with physical and chemical indexes (Ying, Liu, & Hui, 2015; Zheng et al., 2019). Furthermore, pre-harvest sprays of hexanal formulations have effectively extended the shelf-life of mangoes, while electronic noses have accurately predicted the freshness of ridgetail white prawn (*Exopalaemon carinicauda*) and mantis shrimps (*Oratosquilla oratoria*), achieving regression coefficients of 0.97 and forecasting accuracy of 91.67 %, respectively (Anusuya et al., 2016; Shao et al., 2018). These studies collectively underscore the efficacy of integrating electronic sensing technologies with advanced data analysis models for rapid, non-destructive food quality assessments, paving the way for broader applications in the seafood industry and beyond.

Machine learning techniques, which simulate the human learning process, endow computer systems with the ability to autonomously learn from data, extract information, and make decisions and predictions without specific programming (Knott, Perez-Cruz, & Defraeye, 2023; Moysiadis et al., 2023; Yun, Liao, Feng, & Ding, 2024). Deep learning, a powerful branch of machine learning, has undergone rapid advancements in recent years (Kayaalp, 2024; Zhang et al., 2022; Zhang et al., 2022; Ko et al., 2023), especially with the breakthroughs in image recognition through convolutional neural networks (CNNs), offering new possibilities for food quality inspection (Liu, Jia, & Xu, 2019; Schreurs et al., 2024; Xu, Liu, & Zhang, 2021). The YOLO algorithm, an efficient object detection framework, identifies features such as texture, color, and shape in images to swiftly and accurately assess food quality (Bai et al., 2024; Sun, Tang, Li, & Tong, 2024; Sun, Wang, & Xue, 2023). It has been successfully applied in various contexts, including soybean pest detection (Tetila et al., 2024; Zhu, Li, Sun, & Han, 2024), fish defect detection (Mohamed et al., 2020; Al Muksit et al., 2022), walnut recognition (Wang et al., 2024; Wang et al., 2024; Selcuk & Tutuncu, 2023), and mold detection on food surfaces (Jubayer et al., 2021; Li et al., 2023; Li et al., 2023).

The YOLO algorithm stands as a seminal advancement in deep learning-based object detection, offering distinct advantages over other methods in the food detection domain. Primarily, YOLO's unparalleled speed and real-time processing capability stem from its novel approach of treating object detection as a single regression problem, allowing simultaneous prediction of bounding boxes and class probabilities, which drastically reduces computational complexity and enhances efficiency on even modest hardware (Sarah, Abdlemadjid, Sarah, Yacine, & Miloud, 2024). Additionally, YOLO's comprehensive training approach, which considers entire images, significantly minimizes background errors and enhances detection accuracy by leveraging contextual information about objects and their surroundings, a marked improvement over region-based methods like Faster RCNN that may miss broader contextual cues (Samma, Al-Azani, Luqman, & Alfarraj, 2024). Furthermore, YOLO's robustness and adaptability across various applications, from natural images to specialized fields such as food quality assessment, underscore its versatility. This adaptability is further bolstered by continuous advancements in the algorithm, such as YOLOv10 (Tian, Deng, Xu, & Wen, 2024).

During shrimp storage, the body color significantly changes over

time (Chen et al., 2023; Dong et al., 2023; Guo et al., 2024), serving as an important sensory indicator of freshness. This provides an opportunity for rapid identification using the YOLO model. Therefore, this study classified the freshness of *Litopenaeus vannamei* stored at 4 °C based on physicochemical indicators such as TVB-N and TVC, as well as the visual images of the shrimp during the storage period. By utilizing YOLOv8 as the foundation for model optimization, the YOLO-Shrimp model was developed for the non-destructive, rapid detection of shrimp freshness and quality, providing a convenient method for the rapid online recognition of *Litopenaeus vannamei* freshness.

2. Materials and methods

2.1. Changes in aquatic product freshness

2.1.1. Sample collection and preparation

The shrimp utilized in this study were *Litopenaeus vannamei*, selected for uniform size and similar body coloration, averaging approximately 45 shrimp per kilogram. These were procured from the Xiashan Seafood Wholesale Market in Zhanjiang City, Guangdong Province, China, and transported to the laboratory under oxygenated conditions to ensure their vitality. In compliance with ethical guidelines for animal treatment, the shrimp were subjected to humane euthanasia, after which a random selection of 3000 individuals was made for the experimental procedures. Stored at a constant temperature of 4 ± 1 °C, each shrimp was subjected to photographic capture at 8 distinct angles at 7:00 AM daily, including dorsal and ventral views from both the left and right lateral perspectives, as well as anterior and posterior oblique views. This process resulted in a daily acquisition of 1800 images per day, which were subsequently utilized for image processing and grayscale value analysis. Furthermore, 3000 shrimp were randomly divided into 10 groups, each consisting of 300 individuals, and maintained at 4 ± 1 °C. Samples for the assessment of TVB-N and TVC were collected at 9:00 AM daily. All operations were conducted under the aforementioned temperature conditions over a period of seven consecutive days. The chemical reagents used throughout the experiment were of analytical grade, ensuring the accuracy and reliability of the experimental outcomes. The rigorous experimental design and adherence to standardized conditions were critical to obtaining data that accurately reflect the freshness indicators of the shrimp.

2.1.2. Determination of TVB-N levels

TVB-N in the shrimp samples was measured using an automatic Kjeldahl nitrogen analyzer, following the National Food Safety Standard for the Determination of Volatile Salt Basic Nitrogen in Food (GB 5009.228-2016). The shrimp samples were ground, and 5 g of the shrimp paste was placed into a distillation tube. Next, 37.5 mL of water was added, and the mixture was shaken to evenly disperse the sample in the solution. After 30 min of soaking, 0.5 g of magnesium oxide was added, and the tube was connected to the distillation apparatus for analysis. The results were expressed as the amount of nitrogen in mg per 100 g of sample.

2.1.3. Determination of the TVC

Microbial colony counts were determined following the National Food Safety Standard for the Microbiological Examination of Food - Enumeration of Colony-Forming Units (GB 4789.2-2022). In a sterile environment, the shrimp were beheaded, and their thymus was removed. A 5 g sample of shrimp meat was placed in a sterile homogenization bag with 45 mL of sterile saline solution. Homogenize for 1 min, followed by a continuous gradient dilution to obtain 1:10, 1:100, and 1:1000 sample dilutions, with each dilution prepared in triplicate. Apply 0.1 mL of each dilution onto nutrient agar plates and evenly spread using the spread plate method. Incubate the plates at 36 °C ± 1 °C for 48 h.

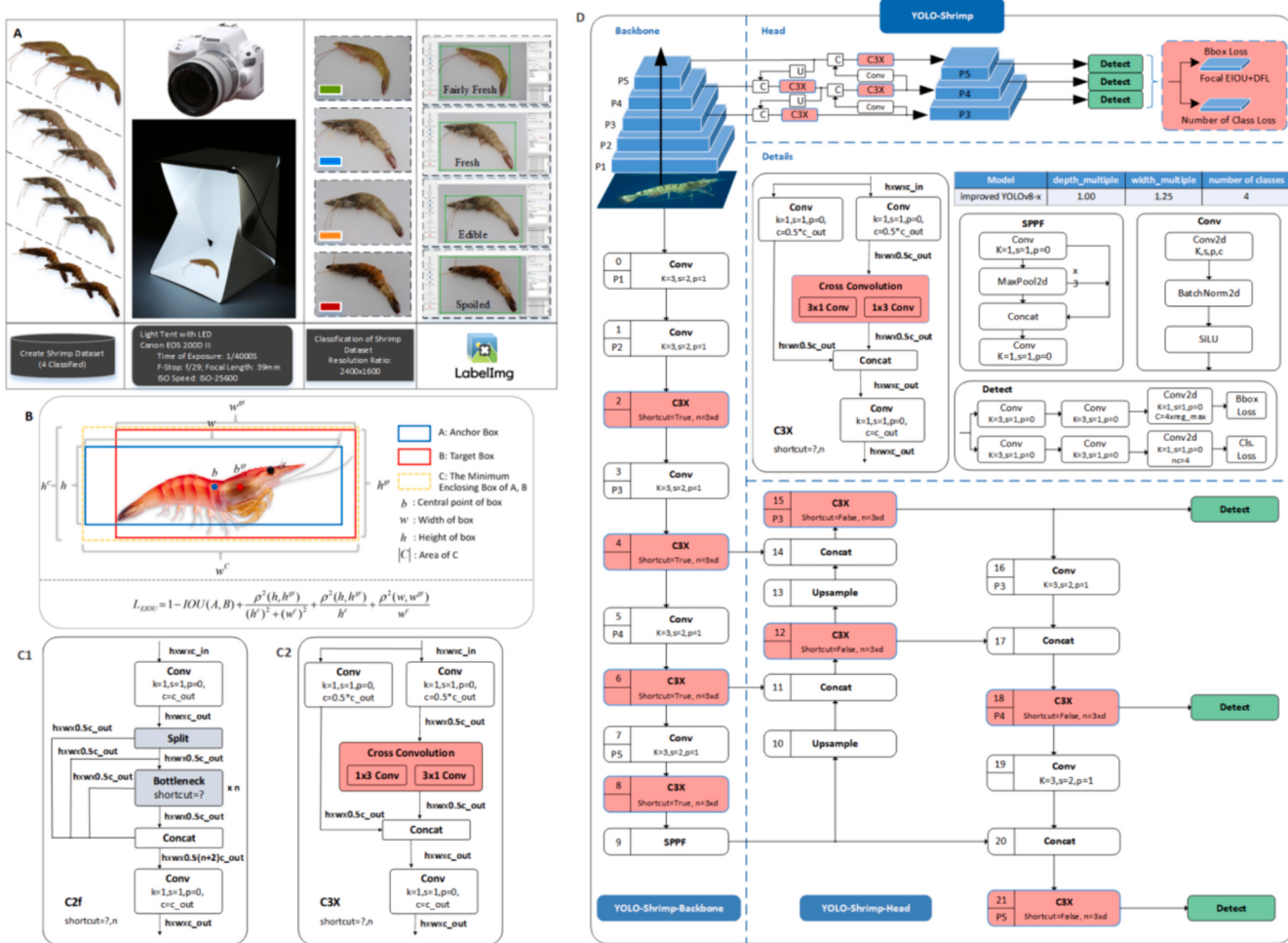


Fig. 1. A: Color alteration process in *Litopenaeus vannamei* during a 7-day storage period; B: EIOU; C1: Structure of the C2f block ($k = (3,3),(3,3)$); C2: Structure of the C3X block ($k = (1,3),(3,1)$); D: YOLO-Shrimp.

2.1.4. Assessment of melanosis

For the grouped experimental samples, images of each shrimp were captured using a Canon EOS 200D II camera (settings: ISO 400, S = 4000) in a state-of-the-art light tent equipped with LED lighting. Imaging was performed under consistent lighting and sterile background conditions to ensure clarity. The images were then processed in ImageJ (version 1.52a, National Institutes of Health) to assess the extent of melanosis in the shrimp.

2.2. Dataset acquisition

In our experiment, photographic images were captured daily for 3000 shrimp, with each shrimp being photographed from 8 distinct perspectives. Specifically, these perspectives included the dorsal and ventral views from both the anterior and posterior sides, as well as from both the left and right lateral sides. Consequently, the daily collection of images summed up to 1800 pictures. Throughout the entire experimental procedure, a total of 12,300 images were carefully selected. These images were subsequently utilized for image processing and the determination of grayscale values. These images are categorized into four distinct freshness quality classifications: "Fairly Fresh", "Fresh", "Edible", and "Spoiled" (see Fig. 1A). Using a state-of-the-art light tent equipped with LED illumination, image acquisition was executed using a Canon EOS 200D II camera. The camera settings were meticulously calibrated, featuring an ultrafast exposure time of 1/4000 s, automated focus mode, a narrow aperture set at f/29, and a high ISO speed of 400 to ensure optimal image clarity. Additionally, the white balance was

adjusted using the camera's sophisticated automatic mode. It is pivotal to note that the entirety of this dataset was captured sans flash, relying solely on a synergistic blend of LED lighting within the photographic tent and ambient indoor lighting conditions. Each image within this comprehensive dataset boasts an impressive resolution of 2400 × 1600 pixels. The annotation process was meticulously executed using the advanced LabelImg annotation software (as depicted in Fig. 1A). This richly detailed dataset, in conjunction with our innovatively optimized YOLO-Shrimp algorithm, stands at the forefront of enhancing computer vision applications, particularly in the nuanced field of shrimp quality assessment.

2.3. The improved YOLOv8 methods

2.3.1. Focal EIoU

The complete IoU (CIoU) loss (Zheng et al., 2005), an advanced metric in the context of object detection tasks within YOLOv8, exhibits several salient features that merit attention in the realm of scientific discourse. The CIoU loss incorporates an innovative geometric framework that surpasses conventional intersection over union (IoU) measures by considering, not only the spatial overlap between the predicted and ground truth bounding boxes, but also their respective aspect ratio and center distance. CIoU loss demonstrates superior robustness in mitigating the issue of bounding box instability during the training process. In this study, a novel extension to the YOLO framework has been presented through the seamless integration of the pioneering focal and efficient IOU (Focal EIoU) loss paradigm. The fundamental impetus

driving this augmentation is the amelioration of the inherent complexities within the object detection endeavors, prominently encompassing the rectification of class imbalance quandaries and the enhancement of precision in bounding box localization. By substituting the traditional IOU-centric loss function with the focal EIoU loss, the extant deficiencies in loss functions are remediated, while the gradients elicited from instances of varying quality levels are concurrently harmonized.

To expedite the targeted accentuation of the EIoU loss upon instances of elevated excellence, the IOU metric has been harnessed to effectuate a scrupulous reconfiguration of the EIoU loss. This endeavor culminates in the derivation of the Focal-EIOU loss formulation as follows:

$$L_{\text{Focal-EIOU}} = \text{IOU}^\gamma L_{\text{EIOU}} \quad (1)$$

where IOU is, the intersection over union and γ , is a parameter used to control the degree of inhibition of the outliers. The L_{EIOU} is defined as in Fig. 1B.

2.3.2. C3X

Fig. 1C1 and C2 show comparisons of the C2f and C3x computation blocks, respectively. The YOLOv8 model leverages a modified CSPDabnet53 backbone architecture, wherein the conventional cross-stage partial (CSP) modules employed in previous iterations of YOLO have been substituted with C2f modules for enhanced feature extraction. The C2f module entails a triple convolutional process culminating in a concatenation operation. As illustrated in Fig. 1C1, there is a noticeable increase in jump connections and split operations. Furthermore, two convolutional connection layers within the neck module were omitted. Notably, the number of C2f blocks within the backbone was adjusted from 3-6-9-3 to 3-6-6-3. In lieu of the previous objects branch, the decoupled classification and regression branches are now in place. The regression branch adopts the integral form notation as introduced in the distribution focal loss (DFL) framework.

The enhanced structure of the C3X block is illustrated in Fig. 1C2. By augmenting the `shadow` attributes of the cross-convolution field, the integration of 1×3 convolution and 3×1 convolution will augment the precision of YOLO-Shrimp detection. Conversely, the C3X module comprises a triumvirate of cross-convolutions, also denoted as asymmetric or spatial shuffling convolutions. These are deemed superior feature extractors when compared to conventional convolutions, particularly in addressing objects of interest at varying orientations, as is the case with ship detection. In essence, within the purview of the original C2f framework, this investigation has replaced the split and bottleneck module with a cross-convolution module while concurrently incorporating the convolution module in the input processing.

2.3.3. Focal EIOU + C3X

YOLOv8 represents the latest iteration within the YOLO paradigm for object detection and image segmentation and was meticulously crafted by the accomplished developers at Ultralytics. YOLOv8 stands as the vanguard of cutting-edge, SOTA (State-of-the-Art) models, ingeniously expanding upon the triumphs of its predecessors in the YOLO lineage, ushering in novel attributes and enhancements designed to increase both its performance and adaptability. This sophisticated model is amenable to extensive training on voluminous datasets and boasts compatibility across a spectrum of hardware platforms, ranging from conventional CPUs to powerful GPUs. Notably, the distinguishing hallmark of YOLOv8 is its innate scalability, which is orchestrated to accommodate an array of operational environments. Furthermore, it is ingeniously architected as a versatile framework, embracing all antecedent iterations of the YOLO model, thereby rendering seamless transitions between versions, and facilitating insightful performance comparisons.

The YOLO-Shrimp methodology, an extension of YOLOv8, is used for precise assessment of freshness and quality in shrimp imagery. The innovative enhancements in YOLO-Shrimp, indicated by the red

Table 1
The hyperparameters for YOLO-Shrimp training.

Hyperparameters	Value
Initial learning rate(lr0)	0.001
Final learning rate(lrf)	0.01
Batch size	16
Epochs	2500
Optimizer	SGD
Input image size	640
Confidence threshold	0.8
Workers	8
Loss function	Focal EIOU

shadows outlined in Fig. 1D, are elucidated as follows:

- **Backbone:** The underlying architecture maintains the essence of Conv, yet it transcends the prior C2f module in YOLOv8 by adopting the C3X module, thereby increasing its precision. In keeping with YOLOv8's framework, YOLO-Shrimp continues to employ the SPPF module and other architectural components.
- **PAN-FPN:** YOLO-Shrimp seamlessly integrates the PAN concept, retaining its foundational principles while distinguishing itself by substituting the C2f module with the C3X module, a differentiation discernible in the structural blueprints when comparing YOLOv8 and YOLO-Shrimp.
- **Decoupled-Head and Anchor-Free:** YOLO-Shrimp advances with the contemporary decoupled structural design in its Head module, effectively segregating the classification and detection components and transitioning from the Anchor-Based methodology to Anchor-Free detection.
- **Loss Function:** YOLO-Shrimp introduces TaskAlignedAssigner, a concept derived from TOOD, and incorporates the Focal EIOU+Distribution Focal Loss (DFL) to enhance the precision of regression loss, enhancing the overall model's robustness and performance (Zhang, Ren, et al., 2022; Zhang, Wei, et al., 2022).

Therefore, the dataset acquisition for Fig. 1A involves high-resolution images (2400×1600 pixels) of *Litopenaeus vannamei*, captured using a Canon EOS 200D II camera in a controlled light tent with LED illumination. These meticulously annotated images, categorized into four freshness classifications: "Fairly Fresh", "Fresh", "Edible", and "Spoiled", form the foundation for enhancing computer vision applications in shrimp quality assessment. The Extended Intersection over Union (EIoU) loss function, depicted with its anchor box, target box, and central point, incorporates CiOU metrics to improve precision in bounding box localization by addressing class imbalance and refining gradient harmonization (Fig. 1B). Structural enhancements include the C2f block with a triple convolutional process for superior feature extraction and the C3X block with cross-convolution fields to enhance detection precision for objects with varying orientations (Fig. 1C2). The YOLO-Shrimp model architecture integrates these innovations in its backbone, PAN-FPN, decoupled-head, and anchor-free methodologies. It adopts the C3X module for increased precision, retains the SPPF module, and introduces TaskAlignedAssigner and Focal EIOU+Distribution Focal Loss (DFL) for enhanced regression loss precision, thereby bolstering the model's robustness and performance (Fig. 1D). These advancements position the YOLO-Shrimp model as a sophisticated tool for non-destructive detection and assessment of shrimp freshness quality.

2.4. Model training and hyperparameters

The YOLO-Shrimp model, an enhanced version of YOLOv8, was trained using a dataset of 12,300 high-resolution images of *Litopenaeus vannamei*. The dataset was split into training (70 %), validation (15 %), and testing (15 %) sets. The model was trained with a batch size of 16

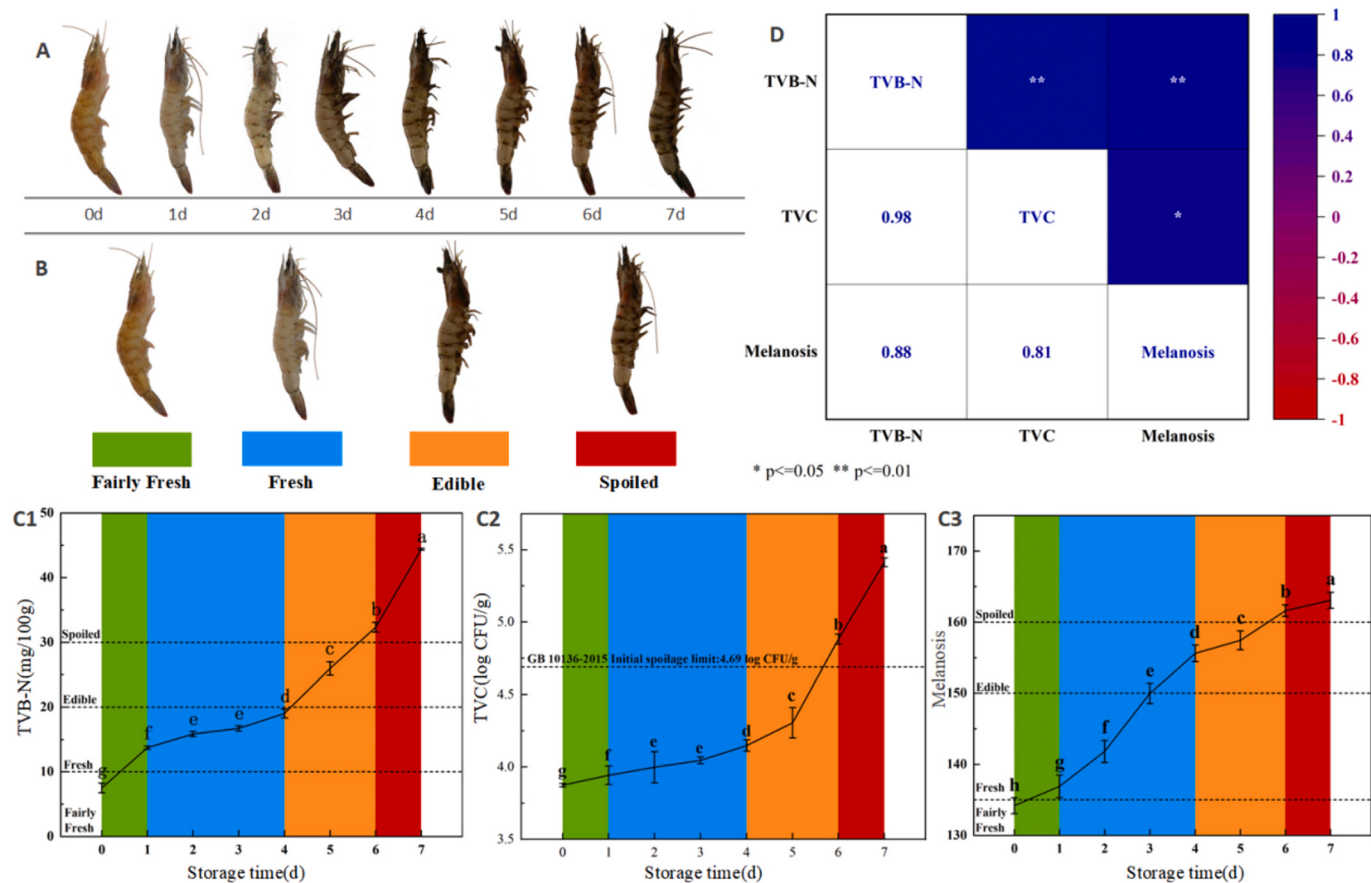


Fig. 2. A: Color alteration process in *Litopenaeus vannamei* during a 7-day storage period; B: Four stages of color transformation in *Litopenaeus vannamei* specimens; C: TVB-N, TVC, and the curve illustrating changes in the degree of melanosis; D: Correlation analysis of TVB-N, TVC, and melanosis, where $0.01 < P < 0.05$ indicates a significant difference, and $P < 0.01$ indicates a highly significant difference.

over 2500 epochs, utilizing a learning rate of 0.001, optimized through stochastic gradient descent (SGD). The input image size was standardized to 640 pixels, and the confidence threshold was set at 0.8 to ensure high detection accuracy (Table 1).

3. Results and discussion

3.1. TVB-N

The accumulation of TVB-N exhibited a gradual increase with the extension of storage time. From Day 0 to Day 4, the increase was slow; however, a significant acceleration in TVB-N accumulation was observed after Day 4, as illustrated in Fig. 2C1. During the storage of shrimp, the rise in TVB-N levels was correlated with a decrease in freshness; freshness was maintained effectively from Day 0 to Day 4, but a notable decline in quality occurred thereafter. This pattern aligns with findings reported by (Yu, Wang, Wen, Yang, & Zhang, 2019), where TVB-N levels in shrimp similarly surged after the fourth day of storage, with some samples surpassing the National Food Safety Standard for Fresh and Frozen Aquatic Products (GB 2733-2015) upper limit by Day 4.

In the present study, the initial TVB-N value for *Litopenaeus vannamei* on Day 0 was recorded at 7.50 mg/100 g. Subsequent measurements on Days 1 through 7 revealed TVB-N values of 13.73, 15.85, 16.73, 19.03, 25.96, 32.31, and 44.38 mg/100 g, respectively. According to the Aquatic Industry Standard for Frozen Shrimp (SC/T 3113-2002) and the National Food Safety Standard for Fresh and Frozen Aquatic Products (GB 2733-2015), the grading criteria based on TVB-N (mg/100 g) are as follows: ≤ 20 for first-grade freshness, $20 < \text{TVB-N} \leq 25$ for second-grade

freshness, $25 < \text{TVB-N} \leq 30$ for third-grade freshness, and > 30 for inedible spoilage. In this study, shrimp freshness was classified as follows: $\text{TVB-N} \leq 10$ for extremely fresh, $10 < \text{TVB-N} \leq 20$ for fresh, $20 < \text{TVB-N} \leq 30$ for edible, and $> 30 \text{ mg}/100 \text{ g}$ for inedible spoilage.

On the fourth day of storage, the TVB-N value reached 19.03 mg/100 g, which, although closed to the 20 mg/100 g threshold between first- and second-grade freshness, marked a significant inflection point where TVB-N began to rise sharply, as shown in Fig. 2C1. Despite the shrimp on Day 4 was categorized as "fresh" based on current TVB-N levels, they were classified as "edible" to better reflect their quality and the potential for rapid deterioration. This classification accounts for the measured TVB-N values as well as the observed trend in quality decline and spoilage risk during subsequent storage. Consequently, the freshness of *Litopenaeus vannamei* in this study was categorized as follows: Day 0, extremely fresh; Days 1–3, fresh; Days 4–5, edible; and Day 6, inedible. These findings are consistent with those reported by (Zhang et al., 2024; Zhou et al., 2023), confirming the applicability of using TVB-N levels for grading shrimp freshness.

3.2. TVC

The variations in the Total Viable Count (TVC) of *Litopenaeus vannamei* during storage were presented in Fig. 2C2. As storage time increased, TVC levels showed a gradual upward trend. During the initial 0–5 days of storage, TVC exhibited a slow increase, followed by a sharp acceleration post-Day 5, which generally corresponded with the overall trend observed for TVB-N. However, it is noteworthy that the growth rate of TVC was slower than that of TVB-N before Day 5. During the "edible" phase, two distinct shifts in TVC growth rate were identified: a

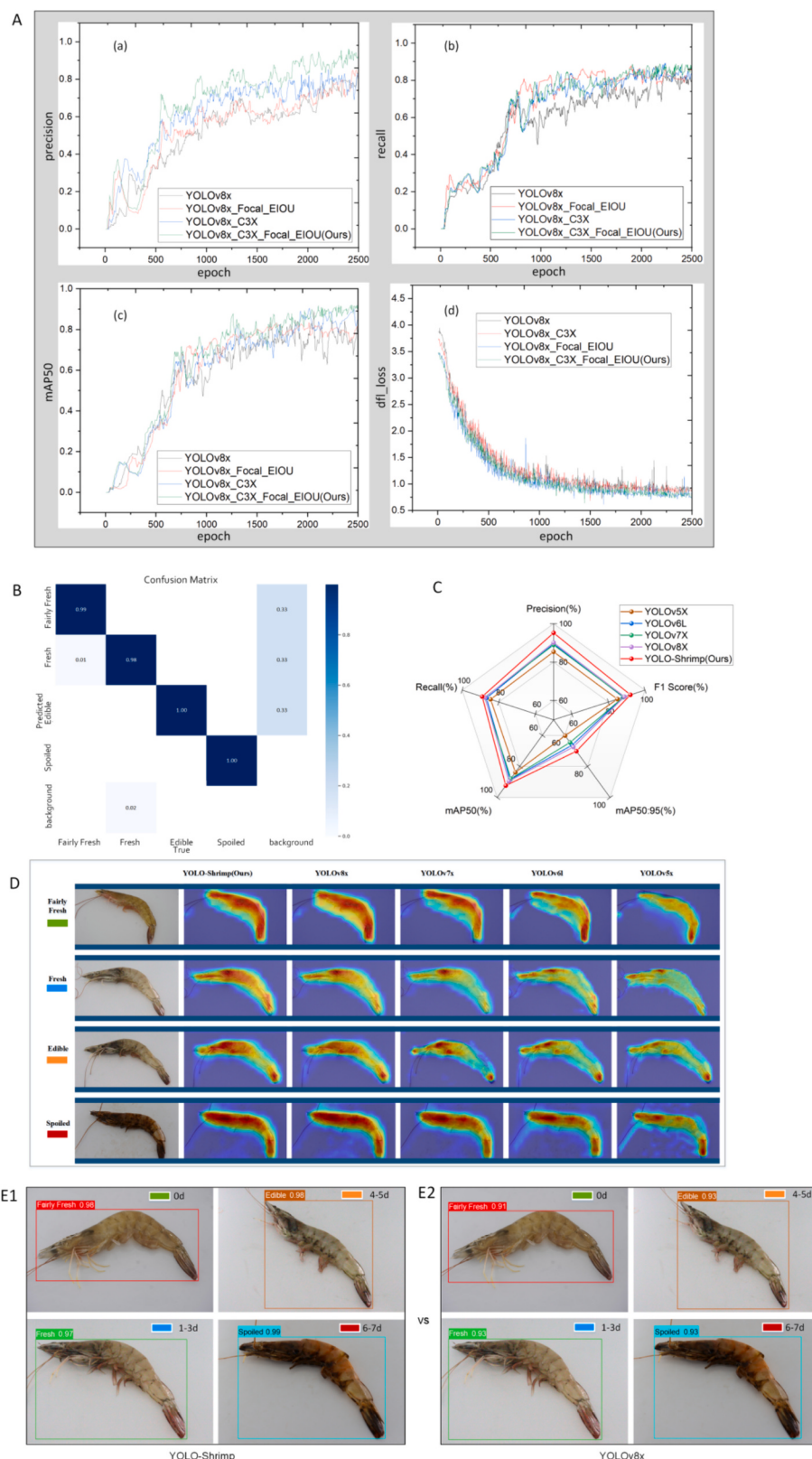


Fig. 3. A: A Comparison of ablation experiments to evaluate the YOLOv8x_C3X_Focal_EIOU model against the original model. (a) precision curve, (b) recall curve, (c) mAP50 curve, and (d) dfl_loss curve. B: Confusion matrix; C: Comparison of the experimental results of Grad-CAM for four kinds of shrimp freshness classifications, visualizing the heatmaps of the proposed YOLO-Shrimp model alongside mainstream object detection models, including YOLOv8x, YOLOv7x, YOLOv6l, and YOLOv5x; D: Radar chart of comparisons with five YOLO algorithms (5000 epochs); E1 and E2: Before and after comparisons of freshness detection of shrimp bodies.

notable increase between Days 4 and 5, followed by a rapid surge after Day 5. This phenomenon can be attributed to the adaptation and growth cycle of microorganisms within the refrigerated environment. Initially, microbial growth can be inhibited due to the time required for adaptation to the new environment. Additionally, endogenous enzymes, such as proteases, remained relatively active even at low temperatures, potentially leading to rapid TVB-N accumulation, while microbial growth is more heavily influenced by environmental conditions (Das & Mishra, 2023). As storage time progresses, microorganisms acclimated to their surroundings and began to proliferate actively, caused an accelerated increase in TVC. This explanation aligns with findings by (Kimbuathong, Leelaphiwat, & Harnkarnsujarit, 2020), who observed that microbial communities experience rapid growth once acclimated to the environment. Furthermore, the accumulation of TVB-N might provide an additional nitrogen source for microorganisms, thereby promoting their growth and contributing to the subsequent acceleration of TVC (Li, Cai, et al., 2023; Li, Zhu, et al., 2023).

On Day 0 of storage, TVC was at its minimum, indicating the freshest state of the shrimp. Microbial levels gradually increased between Days 1 and 3, became noticeably higher between Days 4 and 5, and experienced a rapid surge after Day 5, as shown in Fig. 2C2. By Day 6, the TVC of the shrimp reached 4.88367 log CFU/g. According to the National Food Safety Standard for Aquatic Products of Animal Origin (GB 10136–2015), the maximum permissible microbial content for shrimp is 4.69 log CFU/g. These findings indicate that the TVC of *Litopenaeus vannamei* surpassed the safe consumption threshold on Day 6 of storage, rendering it inedible. This observation is consistent with the study conducted by Laorenza (Laorenza & Harnkarnsujarit, 2023) on total viable counts.

3.3. Melanosis

During shrimp storage, melanosis (blackening) occurred as a result of the catalytic activity of polyphenol oxidase (PPO) within the shrimp. PPO oxidized phenolic compounds into quinones, which subsequently underwent nonenzymatic reactions to form melanin, leading to the darkening of the shrimp exoskeleton. Melanosis initially manifested in the cephalothorax region and progressively intensified with prolonged storage, eventually spreading to the tail, legs, and other body parts Kimbuathong (Kimbuathong et al., 2020).

The degree of melanosis could be quantified through the grayscale value in image analysis, which reflected the darkness of the shrimp meat and indirectly indicates its freshness. Grayscale values range from 0 to 255, with 0 representing pure black, 255 representing pure white, and intermediate values corresponding to varying shades of gray. In this study, the inverse color method of ImageJ was employed, where a higher melanosis level corresponded to a higher grayscale value.

Following storage at 4 ± 1 °C, the degree of melanosis exhibited temporal changes. The grayscale value, as a quantification metric, showed a notable upward trend during the first 0–4 days, indicated a deepening color of the shrimp and a decline in freshness (Fig. 2C3). After Day 4, the growth rate of the grayscale value slowed but continued to rise, reaching a relatively high level after Day 6, suggesting significant darkening and a substantial loss of freshness. This pattern aligns with the findings of Basiri (Basiri, Shekarforoush, Aminlari, & Akbari, 2015) and Kimbuathong (Kimbuathong et al., 2020).

Specifically, as illustrated in Fig. 2C3, the grayscale value on Day 0 was 134.1, which increased to 136.92, 141.81, and 149.96 on Days 1, 2, and 3, respectively, indicating a trend toward darkening shrimp color. By Days 4 and 5, the values further increased to 155.62 and 157.44, respectively. On Day 6, the value exceeded 160, and based on the TVB-N and TVC assessments, it is concluded that when the grayscale value surpasses 160, the shrimp meat was spoiled and inedible. The grayscale ranges for the different freshness levels, based on TVB-N and TVC evaluations, were as follows:

- Extremely fresh: Grayscale value ≤ 135 . On Day 0, the shrimp meat was usually light-colored and at its freshest.
- Fresh: $135 < \text{Grayscale value} \leq 150$. On Days 1, 2, and 3, the shrimp color darkened slightly, but good freshness was retained.
- Edible: $150 < \text{Grayscale value} \leq 160$. On Days 4 and 5, the color deepened further, and freshness declined, but the shrimp remained edible.
- Spoiled/Inedible: Grayscale value > 160 . From Day 6 onward, the meat color became significantly darker, indicating a substantial freshness loss and making the shrimp unfit for consumption.

Monitoring the changes in the degree of melanosis in *Litopenaeus vannamei* during storage provided valuable data for training the YOLO-Shrimp model. By analyzing changes in grayscale values as a quantitative indicator of melanosis, the model could learn to identify patterns in shrimp meat color changes and effectively classify freshness levels.

3.4. Correlation analysis

To elucidate the relationship between different indicators in assessing shrimp freshness, a correlation analysis was performed between TVB-N, TVC, and grayscale values based on the obtained results. As illustrated in Fig. 2D, the visual changes (gray value of shrimp) exhibited a positive correlation with the changes in TVB-N and TVC, with correlation coefficients of 0.88 and 0.81, respectively.

This correlation is attributed to the intensification of microbial growth and enzymatic activity as storage duration extends. During this period, microorganisms, through their metabolic activities, activate the endogenous polyphenol oxidase (ProPPO) in shrimp. ProPPO oxidizes phenolic compounds into quinones, which subsequently engage in non-enzymatic reactions to form melanin, leading to the darkening of the shrimp's exoskeleton and a deepening of meat color, thus resulting in an increase in grayscale values (Kimbuathong et al., 2020).

Furthermore, the metabolic byproducts of microorganisms, particularly the degradation of proteins into ammonia and other volatile nitrogen compounds through microbial and enzymatic actions, contribute to the accumulation of TVB-N. This accumulation demonstrates a significant positive correlation with the rise in grayscale values. These findings indicate that the grayscale value, serving as an intuitive and non-destructive indicator, effectively reflects the biochemical changes occurring in shrimp meat during storage and is closely connected to the quantitative biochemical indicators of TVB-N and TVC.

Consequently, the grayscale value is identified as an effective and reliable metric for assessing shrimp freshness. The YOLO-Shrimp model, having been trained on a substantial dataset of images, demonstrates the ability to learn the specific characteristics associated with shrimp freshness. This capability facilitates the model's ability to conduct rapid and precise freshness analysis and grading, thereby providing a robust scientific foundation for the non-destructive detection and assessment of shrimp quality.

3.5. Ablation study and comparative analysis

Ablation studies compared the performance of YOLOv8x, YOLOv8x_C3X, YOLOv8x_Focal_EIOU, and the combined YOLO-Shrimp model. The YOLO-Shrimp model demonstrated superior performance, with precision, recall, F1 score, and mAP50 significantly improved over the baseline YOLOv8x model (Fig. 3A). Precision increased from 83.39 % to 93.93 %, recall from 82.55 % to 88.17 %, F1 score from 84.21 % to 91.67 %, and dlf_loss decreased by 8.14 %.

Confusion matrix confirmed the YOLO-Shrimp model's high accuracy in classifying shrimp freshness levels (Fig. 3B). Notably, "spoiled" and "edible" shrimp were detected with 100 % accuracy. The Grad-CAM heatmaps further illustrated the model's focus areas, with the YOLO-Shrimp model showing superior detection across all freshness categories compared to YOLOv8x, YOLOv7x, YOLOv6l, and YOLOv5x.

Table 2

Comparison of improved YOLO-Shrimp model performances with other common AI detection methods.

Models	Stage Detectors	Precision (%)	Recall (%)	F1 Score (%)	mAP50 (%)	mAP50:95 (%)
Fast R-CNN	Two-Stage	64.32	65.67	64.99	61.26	43.98
Faster R-CNN	Two-Stage	71.36	73.83	72.57	63.38	45.36
R-FCN	Two-Stage	72.33	75.92	74.08	67.84	47.98
FPN	Two-Stage	80.58	81.63	81.1	74.47	57.36
YOLOv5X	One-Stage	85.4	84.45	84.92	83.78	60.21
YOLOv6L	One-Stage	89.53	86.73	88.11	88.56	66.32
YOLOv7X	One-Stage	88.97	87.68	88.32	87.83	64.58
YOLOv8X	One-Stage	90.16	87.47	88.79	89.48	67.47
YOLO-Shrimp (Ours)	One-Stage	95.23	89.05	92.04	92.32	70.2

(Fig. 3D).

3.6. Comparison with other shrimp recognition methods

When comparing the YOLO-Shrimp model with other YOLO models (YOLOv5X, YOLOv6L, YOLOv7X, YOLOv8X) and several two-stage detection models (Fast R-CNN, Faster R-CNN, R-FCN, and FPN), the YOLO-Shrimp model demonstrated superior performance. Specifically, it exhibited the highest precision (95.23 %), recall (89.05 %), F1 score (92.04 %), mAP50 (92.32 %), and mAP50:95 (70.2 %) after 5000 epochs of training (Table 2, Fig. 3C). This exceptional performance highlights the robustness and effectiveness of the YOLO-Shrimp model in non-destructive freshness detection, as evidenced by the radar chart comparison (Fig. 3D).

In addition, the two-stage detectors, including Fast R-CNN, Faster R-CNN, R-FCN, and FPN, while significant in the object detection domain, generally resulted in lower performance metrics compared to the YOLO-Shrimp model. Fast R-CNN achieved a precision of 64.32 %, recall of 65.67 %, F1 score of 64.99 %, mAP50 of 61.26 %, and mAP50:95 of 43.98 %. Faster R-CNN showed better results with a precision of 71.36 %, recall of 73.83 %, F1 score of 72.57 %, mAP50 of 63.38 %, and mAP50:95 of 45.36 %. R-FCN recorded a precision of 72.33 %, recall of 75.92 %, F1 score of 74.08 %, mAP50 of 67.84 %, and mAP50:95 of 47.98 %. FPN, the highest performer among two-stage detectors,

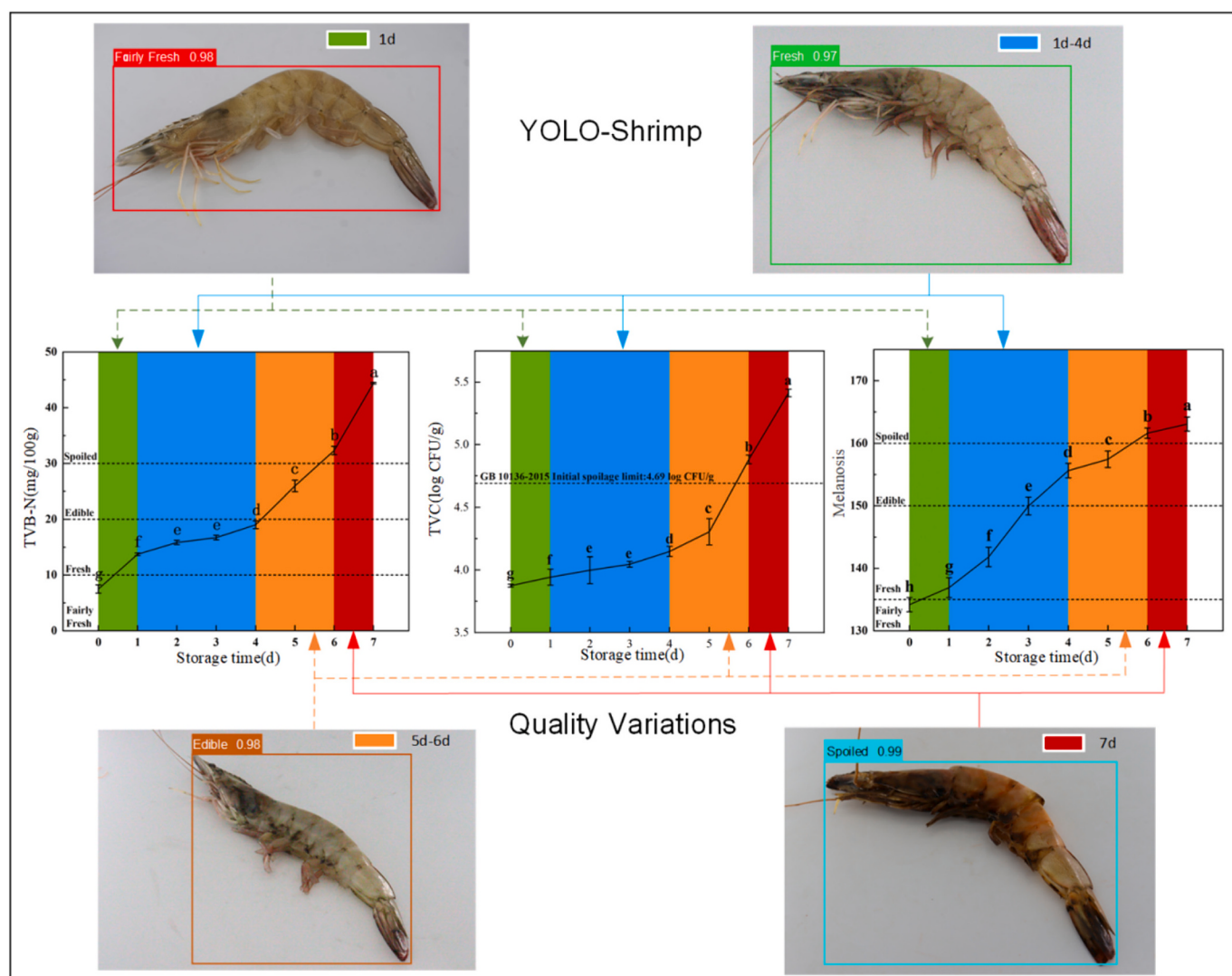


Fig. 4. The relationship between the detection outcomes of the YOLO-Shrimp model and the quality variations observed over a period of seven days.

demonstrated a precision of 80.58 %, recall of 81.63 %, F1 score of 81.1 %, mAP50 of 74.47 %, and mAP50:95 of 57.36 %. Despite these improvements, the YOLO-Shrimp model outperformed all two-stage detectors across all key metrics. This comparison underscores the YOLO-Shrimp model's superiority in efficiency and effectiveness for rapid, non-destructive shrimp freshness detection, setting a new standard in the seafood industry's quality control and safety assurance.

3.7. Detection relationship and practical implications

The YOLO-Shrimp model's detection confidence closely aligned with biochemical and microbiological indicators. On Day 0, the model detected "Fairly Fresh" shrimp with 98 % confidence, correlating with low TVB-N (7.504–13.734 mg/100 g) and TVC (3.875–3.943 CFU/g) values. For "Fresh" shrimp (Days 1–3), "Edible" shrimp (Days 4–5), and "Spoiled" shrimp (Day 6), the model's classifications matched the corresponding TVB-N, TVC, and melanosis metrics (Fig. 4).

The YOLO-Shrimp model's advancements have substantial implications for the seafood industry, enhancing quality control, supply chain management, and regulatory compliance. The model's non-destructive, rapid detection capabilities ensure that high-quality shrimp reaches consumers, improving customer satisfaction and supporting food safety standards. This model can also be adapted for other perishable foods, enhancing non-destructive detection methods across the food industry. Similar non-destructive testing methods for food optimized with YOLO models include fish quality testing (Akgul, Kaya, & Zencir Tanir, 2023), apple ripeness identification (Xiao, Nguyen, & Yan, 2024), mildew detection in rice grains (Sun et al., 2024), and so on.

4. Conclusion

In conclusion, the YOLO-Shrimp model, a refined iteration of the YOLOv8 architecture with an integrated focal EIOU loss function and C3X computation module, has demonstrated significant advancements in the nondestructive, rapid detection of freshness in *Litopenaeus vannamei*. This study validated the efficacy of the model through robust empirical evidence, showing its consistency with biochemical, microbiological, and physical indicators of shrimp quality. The precision enhancements in model performance, evidenced by improved metrics such as precision, recall, F1 score, and mAP50, underscore its potential to revolutionize standards in food safety and quality control within the seafood industry. The model's ability to accurately evaluate the freshness of shrimp through a detailed analysis of texture, color, and morphological features offers a substantial advantage in enhancing the operational efficiency and reliability of seafood freshness assessments. Ultimately, the YOLO-Shrimp model has emerged as a superior technological innovation, setting a new benchmark for the industry in maintaining the highest standards of food safety and consumer satisfaction. Future research will focus on expanding the study of seafood freshness quality variations and integrating diverse machine learning algorithms to further enhance non-destructive detection methods. Developing standalone mobile applications and detection instruments will broaden the technology's accessibility and practicality, ensuring its wider adoption in food safety and quality control.

CRediT authorship contribution statement

Mingxin Hou: Writing, Conceptualization, Methodology, Data curation. **Xiaowen Zhong:** Writing – original draft, Visualization. **Ouyang Zheng:** Writing – review & editing, Supervision, Resources, Conceptualization. **Qinxiu Sun:** Writing – review & editing, Formal analysis. **Shucheng Liu:** Project administration. **Mingxin Liu:** Methodology, Data curation, Conceptualization.

Declaration of competing interest

The authors disclose no financial conflicts of interest or personal affiliations that could bias the findings presented in this manuscript.

Data availability

Data will be made available on request.

Acknowledgments

The authors would like to thank the reviewers and editors for their time to help improve this paper.

This research was supported in part by the Natural Science Foundation of China (62171143), the Special Fund for Scientific and Technological Innovation Strategy of Guangdong Province (2022A05036), the Fund of Guangdong Provincial Key Laboratory of Intelligent Equipment for South China Sea Marine Ranching (2023B1212030003), Guangdong Higher Education Association's "14th Five Year Plan" 2024 Higher Education Research Project(47) and Special Fund for Basic Research Business Expenses of the Chinese Academy of Tropical Agricultural Sciences (1630132024004).

References

- Akgul, I., Kaya, V., & Zencir Tanir, O. (2023). A novel hybrid system for automatic detection of fish quality from eye and gill color characteristics using transfer learning technique. *PLoS One*, 18(4), 1–15. <https://doi.org/10.1371/journal.pone.0284804>
- Al Muksit, A. F., Hasan, F., Emon, H. B., Haque, M. R., Anwary, A. R., & Shatabda, S. (2022). YOLO-fish: A robust fish detection model to detect fish in realistic underwater environment. *Ecological Informatics*, 72, Article 101847. <https://doi.org/10.1016/j.ecoinf.2022.101847>
- Anusuya, P., Nagaraj, R., Janavi, G. J., Subramanian, K. S., Paliyath, G., & Subramanian, J. (2016). Pre-harvest sprays of hexanal formulation for extending retention and shelf-life of mango (*Mangifera indica L.*) fruits. *Scientia Horticulturae*, 211, 231–240. <https://doi.org/10.1016/j.scienta.2016.08.020>
- Bai, B. Y., Wang, J. S., Li, J. L., Yu, L., Wen, J. T., & Han, Y. X. (2024). T-YOLO: A lightweight and efficient detection model for nutrient buds in complex tea-plantation environments. *Journal of the Science of Food and Agriculture*, 104(10). <https://doi.org/10.1002/jsfa.13396>
- Basiri, S., Shekarforoush, S. S., Aminlari, M., & Akbari, S. (2015). The effect of pomegranate peel extract (PPE) on the polyphenol oxidase (PPO) and quality of Pacific white shrimp (*Litopenaeus vannamei*) during refrigerated storage. *LWT- Food Science and Technology*, 60(2), 1025–1033. <https://doi.org/10.1016/j.lwt.2014.10.043>
- Chen, M. M., Li, B. H., Wu, Y., He, Z., Xiong, X. B., Han, W. D., ... Yang, S. B. (2023). Intelligent biogenic pH-sensitive and amine-responsive color-changing label for real-time monitoring of shrimp freshness. *Journal of the Science of Food and Agriculture*, 103(15), 7798–7808. <https://doi.org/10.1002/jsfa.12856>
- Das, J., & Mishra, H. N. (2023). A comprehensive review of the spoilage of shrimp and advances in various indicators/sensors for shrimp spoilage monitoring. *Food Research International*, 173(1), Article 113270. <https://doi.org/10.1016/j.foodres.2023.113270>
- Dong, Y., Sun, W. L., Li, W. B., Li, L. Y., Xia, F., Wu, L. L., ... Sun, W. X. (2023). Poly-L-lactic acid/lead(II) acetate basic colour indicator membrane for visual monitoring in shrimp freshness. *Packaging Technology and Science*, 36(6), 473–481. <https://doi.org/10.1002/pts.2723>
- Guo, C., Fan, Y. C., Wu, Z. X., Li, D. Y., Liu, Y. X., & Zhou, D. Y. (2024). Effects of edible organic acid soaking on color, protein physicochemical, and digestion characteristics of ready-to-eat shrimp upon processing and sterilization. *Foods*, 13(3), Article 388. <https://doi.org/10.3390/foods13030388>
- Jian, L., Hailin, F., Wei, L., Yuanyuan, G., & Guohua, H. (2016). Design of A Portable Electronic Nose system and Application in K Value Prediction for Large Yellow Croaker(*Pseudosciaena crocea*). *Food Analytical Methods*, 9(10), 2943–2952. <https://doi.org/10.1007/s12161-016-0431-8>
- Jubayer, F., Soeb, J. A., Mojumder, A. N., Paul, M. K., Barua, P., Kayshar, S., ... Islam, A. (2021). Detection of mold on the food surface using YOLOv5. *Current Research in Food Science*, 4, 724–728. <https://doi.org/10.1016/j.crfcs.2021.10.003>
- Kayaalp, K. (2024). A deep ensemble learning method for cherry classification. *European Food Research and Technology*, 250(5), 1513–1528. <https://doi.org/10.1007/s00217-024-04490-3>
- Kimbuathong, N., Leelaphiwat, P., & Harnkarnsujarit, N. (2020). Inhibition of melanosis and microbial growth in Pacific white shrimp (*Litopenaeus vannamei*) using high CO₂ modified atmosphere packaging. *Food Chemistry*, 312, Article 126114. <https://doi.org/10.1016/j.foodchem.2019.126114>
- Knott, M., Perez-Cruz, F., & Defraeye, T. (2023). Facilitated machine learning for image-based fruit quality assessment. *Journal of Food Engineering*, 345, Article 111401. <https://doi.org/10.1016/j.jfoodeng.2022.111401>

- Ko, E., Jeong, K., Oh, H., Park, Y., Choi, J., & Lee, E. (2023). A deep learning-based framework for predicting pork preference. *Current Research in Food Science*, 6, Article 100495. <https://doi.org/10.1016/j.crfcs.2023.100495>
- Laorenza, Y., & Harmkarnsujarit, N. (2023). Ginger oil and lime peel oil loaded PBAT/PLA via cast-extrusion as shrimp active packaging: Microbial and melanosis inhibition. *Food Packaging and Shelf Life*, 38, Article 101116. <https://doi.org/10.1016/j.fpsl.2023.101116>
- Le, Z., Gao, Y. Y., Zhang, J. F., Li, J., Yu, Y., & Hui, G. H. (2016). Chinese quince (*Cydonia oblonga* miller) freshness rapid determination method using surface acoustic wave resonator combined with electronic nose. *International Journal of Food Properties*, 19 (12), 2623–2634. <https://doi.org/10.1080/10942912.2016.1169285>
- Li, K. Y., Zhu, X. Y., Qiao, C., Zhang, L. X., Gao, W., & Wang, Y. (2023). The gray Mold spore detection of cucumber based on microscopic image and deep learning. *Plant Phenomics*, 5, Article 0011. <https://doi.org/10.34133/plantphenomics.0011>
- Li, X. X., Cai, M. R., Li, M. S., Wei, X. Q., Liu, Z., Wang, J. S., ... Han, Y. X. (2023). Combining Vis-NIR and NIR hyperspectral imaging techniques with a data fusion strategy for the rapid qualitative evaluation of multiple qualities in chicken. *Food Control*, 145, Article 109416. <https://doi.org/10.1016/j.foodcont.2022.109416>
- Liu, Y., Zhang, F. X., Zhu, B. W., Ruan, X. R., Yi, X. M., Li, J., ... Hui, G. H. (2020). Effect of sodium lactate coating enriched with nisin on beef strip loins (*M. longissimus lumborum*) quality during cold storage and electronic nose rapid evaluation. *Journal of Food Measurement and Characterization*, 14(6), 2998–3009. <https://doi.org/10.1007/s11694-020-00548-4>
- Liu, Z. H., Jia, X. J., & Xu, X. S. (2019). Study of shrimp recognition methods using smart networks. *Computers and Electronics in Agriculture*, 165, Article 104926. <https://doi.org/10.1016/j.compag.2019.104926>
- Mohamed, H. E., Fadil, A., Anas, O., Wageeh, Y., ElMasry, N., Nabil, A., & Atia, A. (2020). Msr-yolo: Method to enhance fish detection and tracking in fish farms. *Procedia Computer Science*, 170, 539–546. <https://doi.org/10.1016/j.procs.2020.03.123>
- Moysiadias, V., Kokkonis, G., Bibi, S., Moscholios, I., Maropoulos, N., & Sarigiannidis, P. (2023). Monitoring mushroom growth with machine learning. *Agriculture-Basel*, 13 (1), Article 223. <https://doi.org/10.3390/agriculture13010223>
- Samma, H., Al-Azani, S., Luqman, H., & Alfarraj, M. (2024). Contrastive-based YOLOv7 for personal protective equipment detection. *Neural Computing & Applications*, 36(5), 2445–2457. <https://doi.org/10.1007/s00521-023-09212-6>
- Sarah, M., Abdlemadjid, M., Sarah, B., Yacine, H., & Miloud, C. E. (2024). Evaluating the effect of super-resolution for automatic plant disease detection: Application to potato late blight detection. *Multimedia Tools and Applications*. <https://doi.org/10.1007/s11042-024-18574-5>
- Schreurs, M., Piampongsant, S., Roncoroni, M., Cool, L., Herrera-Malaver, B., Vanderaea, C., TheSSeling, F., Kreft, L., Botzki, A., Malcorps, P., Daenen, L., Wenseleers, T., & Verstrepen, K. (2024). Predicting and improving complex beer flavor through machine learning. *Nature Communications*, 15(1). <https://doi.org/10.1038/s41467-024-46346-0>
- Selcuk, T., & Tutuncu, M. (2023). A raspberry pi-guided device using an ensemble convolutional neural network for quantitative evaluation of walnut quality. *Traitement Du Signal*, 40(5), 2283–2289. <https://doi.org/10.18280/ts.400546>
- Shao, C. N., Zheng, H. N., Zhou, Z. X., Li, J., Lou, X. W., Hui, G. H., & Zhao, Z. D. (2018). Ridge tail white prawn (*Exopalaemon carinicauda*) K value predicting method by using electronic nose combined with non-linear data analysis model. *Food analytical methods*, 11(11), 3121–3129. <https://doi.org/10.1007/s12161-018-1297-8>
- Sun, H., Wang, B. Q., & Xue, J. L. (2023). YOLO-P: An efficient method for pear fast detection in complex orchard picking environment. *Frontiers in Plant Science*, 13, Article 108945. <https://doi.org/10.3389/fpls.2022.108945>
- Sun, K., Tang, M. D., Li, S., & Tong, S. Y. (2024). Mildew detection in rice grains based on computer vision and the YOLO convolutional neural network. *Food Science & Nutrition*, 12(2), 860–868. <https://doi.org/10.1002/fsn3.3798>
- Tetila, E. C., Silveira, F. A. G. d., Costa, A. B. d., Amorim, W. P., Astolfi, G., Pistori, H., & Barbedo, J. G. A. (2024). YOLO performance analysis for real-time detection of soybean pests. *Smart Agricultural Technology*, 7. <https://doi.org/10.3389/10.1016/j.atch.2024.100405>
- Tian, Y. Q., Deng, N., Xu, J., & Wen, Z. G. (2024). A fine-grained dataset for sewage outfalls objective detection in natural environments. *Scientific Data*, 11(1), Article 724. <https://doi.org/10.1038/s41597-024-03574-9>
- Wang, H., He, H. J., Ma, H. J., Chen, F. S., Kang, Z. L., Zhu, M. M., ... Zhu, R. G. (2019). LW-NIR hyperspectral imaging for rapid prediction of TVC in chicken flesh. *International Journal of Agricultural and Biological Engineering*, 12(3), 180–186. <https://doi.org/10.25165/j.ijabe.20191203.4444>
- Wang, H. D., Shao, L. T., Zhang, J. H., Xu, X. L., Li, J. J., & Wang, H. H. (2024). Insight into the spoilage heterogeneity of meat-borne bacteria isolates with high-producing collagenase. *Food Science and Human Wellness*, 13(3), 1402–1409. <https://doi.org/10.26599/FSHW.2022.9250118>
- Wang, S., Huang, S. L., Han, Y. Y., Wu, J., Jiao, T. H., Wei, J., ... Chen, Q. S. (2023). Applications of colorimetric sensors for non-destructive predicting total volatile basic nitrogen (TVB-N) content of Fujian oyster (*Crassostrea angulata*). *Food Control*, 153, Article 109914. <https://doi.org/10.1016/j.foodcont.2023.109914>
- Wang, Y. B., Zhang, C. Y., Wang, Z. M., Liu, M. D., Zhou, D., & Li, J. F. (2024). Application of lightweight YOLOv5 for walnut kernel grade classification and endogenous foreign body detection. *Journal of Food Composition and Analysis*, 127, Article 105964. <https://doi.org/10.1016/j.jfca.2023.105964>
- Xiao, B. J., Nguyen, M., & Yan, W. Q. (2024). Apple ripeness identification from digital images using transformers. *Multimedia Tools and Applications*, 83(3), 7811–7825. <https://doi.org/10.1007/s11042-023-15938-1>
- Xu, J. Y., Liu, K. W., & Zhang, C. (2021). Electronic nose for volatile organic compounds analysis in rice aging. *Trends in Food Science & Technology*, 109, 83–93. <https://doi.org/10.1016/j.tifs.2021.01.027>
- Ying, X. G., Liu, W., & Hui, G. H. (2015). Litchi freshness rapi. d non-destructive evaluating method using electronic nose and non-linear dynamics stochastic resonance model. *Bioengineered*, 6(4), 218–221. <https://doi.org/10.1080/21655979.2015.1011032>
- Ying, X. G., Liu, W., Hui, G. H., & Fu, J. (2015). E-nose based rapid prediction of early mouldy grain using probabilistic neural networks. *Bioengineered*, 6(4), 222–226. <https://doi.org/10.1080/21655979.2015.1022304>
- Yu, X. J., Wang, J. P., Wen, S. T., Yang, J. Q., & Zhang, F. F. (2019). A deep learning based feature extraction method on hyperspectral images for nondestructive prediction of TVB-N content in Pacific white shrimp (*Litopenaeus vannamei*). *Biosystems Engineering*, 178, 244–255. <https://doi.org/10.1016/j.biosystemseng.2018.11.018>
- Yun, B. N., Liao, X. Y., Feng, J. S., & Ding, T. (2024). Machine learning-enabled prediction of antimicrobial resistance in foodborne pathogens. *CYTA Journal of Food*, 22(1), Article 2324024. <https://doi.org/10.1080/19476337.2024.2324024>
- Zhang, W., Han, Y. Y., Yang, S., Wang, S., Wu, J., Jiao, T. H., ... Chen, Q. S. (2024). Non-destructive prediction of total volatile basic nitrogen (TVB-N) content of *Litopenaeus vannamei* using A bi-channel data acquisition of colorimetric sensing array. *Journal of Food Composition and Analysis*, 128, Article 106026. <https://doi.org/10.1016/j.jfca.2024.106026>
- Zhang, Y. A., Wei, C. C., Zhong, Y., Wang, H. D., Luo, H., & Weng, Z. Q. (2022). Deep learning detection of shrimp freshness via smartphone pictures. *Journal of Food Measurement and Characterization*, 16(5), 3868–3876. <https://doi.org/10.1007/s11694-022-01473-4>
- Zhang, Y. F., Ren, W. Q., Zhang, Z., Jia, Z., Wang, L., & Tan, T. N. (2022). Focal and efficient IOU loss for accurate bounding box regression. *Neurocomputing*, 506, 146–157. <https://doi.org/10.1016/j.neucom.2022.07.042>
- Zheng, H. N., Wang, S. Y., Ping, X. Y., Shao, C. N., Zhou, H. M., Xiang, B., ... Hui, G. H. (2019). Study of Spinyhead croaker (*Collichthys lucidus*) fat content forecasting model based on electronic nose and non-linear data resolution model. *Food Analytical Methods*, 12(9), 1927–1937. <https://doi.org/10.1007/s12161-019-01510-x>
- Zheng, Z. H., Wang, P., Ren, D. W., Liu, W., Ye, R. G., Hu, Q. H., & Zuo, W. M. (2005). Enhancing geometric factors in model learning and inference for object detection and instance segmentation. *IEEE Transactions on Cybernetics*, 52(8), 8574–8586. <https://doi.org/10.1109/TCYB.2021.3095305>
- Zhou, Y. H., Jiao, L. Z., Wu, J. W., Zhang, Y. H., Zhu, Q. Z., & Dong, D. M. (2023). Non-destructive and in-situ detection of shrimp freshness using mid-infrared fiber-optic evanescent wave spectroscopy. *Food Chemistry*, 422, Article 136189. <https://doi.org/10.1016/j.foodchem.2023.136189>
- Zhu, L. Q., Li, X. M., Sun, H. M., & Han, Y. P. (2024). Research on CBF-YOLO detection model for common soybean pests in complex environment. *Computers and Electronics in Agriculture*, 216, Article 108515. <https://doi.org/10.1016/j.compag.2023.108515>